Journal of Imaging Science and Technology® 61(5): 050401-1–050401-11, 2017.
© Society for Imaging Science and Technology 2017

Real-Time Jet Failure Detection of Inkjet Heads with 1024 Ejectors

Kye-Si Kwon▲ and Jaeryul Yu
Department of Mechanical Engineering, Soonchunhyang University, 22, Soonchunhyang-Ro, Shinchang, Asan, Chungnam, 336-745, South Korea
E-mail: kskwon@sch.ac.kr

Thanh Huy Phung
Department of Electronic Materials and Devices Engineering, Soonchunhyang University, 22, Soonchunhyang-Ro, Shinchang, Asan, Chungnam, 336-745, South Korea

Abstract. *Recently, inkjet-printing industry demands high-speed and single-pass printing that requires simultaneous jetting of a large number of ejectors. As a result, the jetting reliability has become an important issue in most industrial inkjet-printing applications. To ensure the jetting reliability, a real-time monitoring of the jetting status is needed. Since the monitoring process should not interrupt the printing process, the monitoring time for all of the nozzles should be less than 1 second. For this purpose, the authors developed two module prototypes to monitor the commercial inkjet heads with 1024 nozzles: (1) a head driver with an internal self-sensing capability; (2) an external monitoring module that can be used for third-party drivers. To deal with a large number of nozzles effectively, the authors are proposing a parallel sensing scheme that can be used to monitor multi-head jetting. Lastly, the authors verified our monitoring scheme by using a drop visualization system for a comparison of the monitoring results with the droplet jetting images.* © *2017 Society for Imaging Science and Technology.*
[DOI: 10.2352/J.ImagingSci.Technol.2017.61.5.050401]

INTRODUCTION

The application of inkjet technology has broadened from desktop printers to various industries.[1] To increase the productivity when using inkjets, recent industrial printing systems may require a single-pass printing system that is based on simultaneous jetting of numerous printheads.[2] As a result, an inkjet system may use more than 100,000 nozzles per system, and the monitoring of each ejector becomes very complex in most industrial printing systems.[3] To monitor the jetting status of each nozzle during the printing process, the monitoring time should be as short as 1 second to avoid an interruption of the process. The previous vision-based measurements of frozen droplet images in flight may not be suitable for the scanning of all the nozzles during the printing process.[1,4–6] Alternatively, to diagnose the head nozzle status, the printed patterns on substrates can be used to determine whether the printed image from a specific nozzle has abnormalities.[7–9] The use of the printed patterns could be an effective method for the initial diagnosis of the inkjet head operation prior to the printing process, but it is difficult to use for real-time jetting monitoring. Note that some of the nozzles in the inkjet heads can become non-jetting condition during the printing process, so it is important to detect the abnormality immediately via real-time monitoring. A recent proposal is to use piezo self-sensing signals to detect inkjet failures efficiently.[10–13] A piezo inkjet head uses a piezo actuator to jet ink droplets. The piezo actuator can also be used to sense the pressure wave of ink inside the inkjet dispenser; this method uses only electrical signals from the inkjet head and does not require any mechanical fixture or hardware. As a result, the hardware could be simple and the position control of the cameras or sensors to measure the jetted droplets from the specific nozzle would not be required. Given this advantage, our group's previous study reported that the monitoring time could be reduced to a duration as short as 1 second for the case of 128 (or 256) nozzles.[12,13]

However, recent inkjet heads comprise 1024 or more ejectors in order to meet high throughput printing requirements. In addition, numerous heads are commonly used for single-pass printing.[2,3] In this article, we have improved the self-sensing-based inkjet monitoring module in order to monitor more than 1024 nozzles without increasing the monitoring time. The proposed method is based on parallel sensing schemes so that many ejectors can be monitored simultaneously. To implement the proposed parallel sensing scheme in a commercial printhead, we developed two types of monitoring modules: (1) an inkjet driver with sensing and monitoring capability, and (2) an external module that can be used in third-party inkjet drivers. The proposed self-sensing monitoring module is based on the low-cost and high-speed scanning methods that are discussed in Ref. 13. Since the sensing module can be quite small, it was possible to integrate it into the existing inkjet drivers without increasing the total size of the driver, whereby the driver itself could perform the monitoring. Alternatively, the advantage of the external module is a wider selection of printing drivers to choose from; for example, a printing-system developer does not need

▲ IS&T Member.

Received Nov. 4, 2017; accepted for publication July 16, 2017; published online Sep. 28, 2017. Associate Editor: Chunghui Kuo.
1062-3701/2017/61(5)/050401/11/$25.00

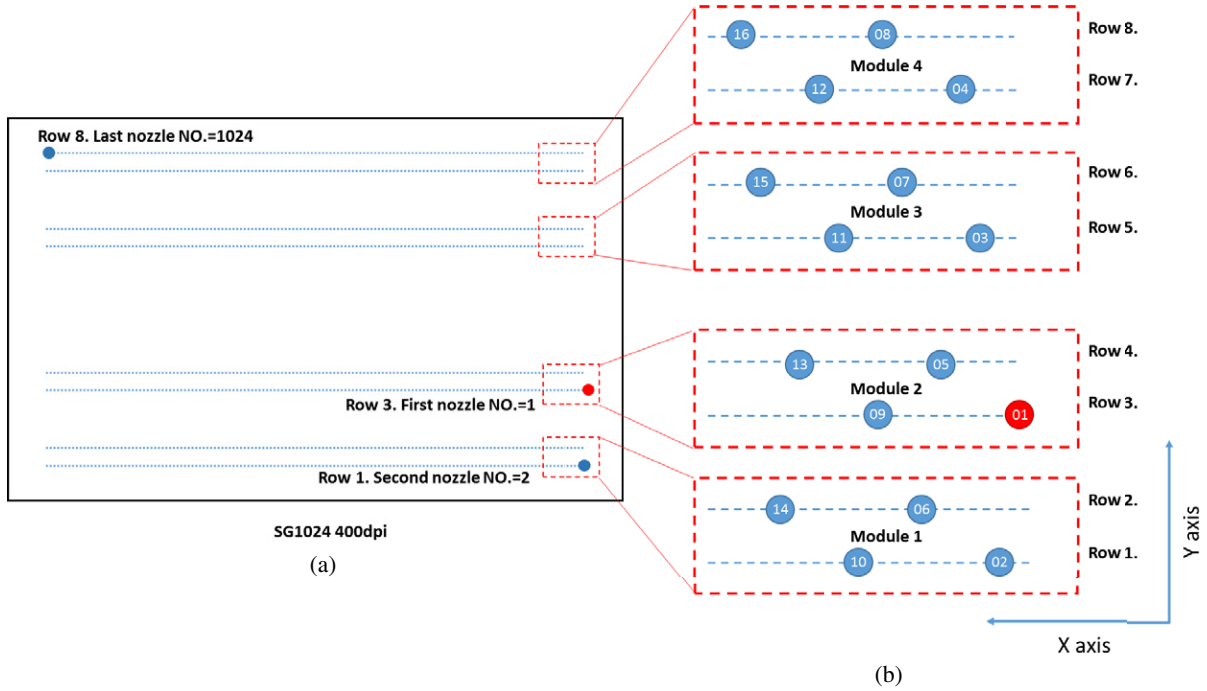

Figure 1. Nozzle scheme for the SG1024 printhead. (a) Nozzle layout. (b) Module layout (magnified nozzle layout).

to replace the existing driver to monitor the jetting status of the head.

A commercially available inkjet head with 1024 ejectors (SG1024, Fujifilm Dimatix, U.S.A.) was used for the feasibility testing of both prototypes. For the verification of the hardware module and the software algorithm, we developed a drop visualization system for the SG1024 to compare the results of the self-sensing monitoring with a vision-based jetting image. The real-time monitoring capability of the proposed self-sensing modules was demonstrated by showing the nozzle-status updates at the setting-time intervals.

Self-sensing Algorithm for 1024 Ejectors

To extract the piezo self-sensing signals from the inkjet head, electronic sensing circuits should be inserted between the driver and the inkjet head. In the authors' previous study, a low-cost and high-speed monitoring method was discussed.[12] To monitor the jetting status of an inkjet head with 128 (or 256) nozzles (S-class and Q-class heads, Fujifilm Dimatix, USA), a bridge circuit was modified to measure the self-sensing components in the electrical currents from two independent drivers.[12,13] Then, a signal-processing algorithm was developed to calculate the nozzle status of the 128 or 256 nozzles.

However, the number of nozzles in the recent inkjet printheads has been increased beyond 1024 nozzles; in addition, the monitoring methods should be extended to multi-head systems. The critical issues for inkjet monitoring might be the requisite monitoring time for the scanning of that many nozzles. For this purpose, a new parallel-based scanning method is being proposed in the present article for simultaneous monitoring of numerous nozzles that can minimize the monitoring time.

For the practical implementation of the proposed method, a commercial head (Fujifilm Dimatix head, model SG1024) was used. The SG1024 printhead is a 400 dpi, 1024-nozzle printhead, with 8 rows of 128 nozzles each, and the spacing of each row is 50 dpi, as shown in Figure 1(a).

Fig. 1(b) shows the nozzle numbering of the SG1024 nozzle layout in Fig. 1(a). The nozzles are numbered sequentially, so that the x-direction distance between the adjacent nozzle numbers can be 0.0635 mm, which corresponds to 400 dpi. For example, the distance between the nozzle numbers 1 and 2 in the x-direction is 0.0635 mm, but the nozzles are not located in the same row. The numbering of the adjacent nozzles in each row differs by a value of 8, so the distance between them is represented by $0.0635 \times 8 = 0.508$ mm.

The nozzles in the same row share the driving voltage from the single driver; eight independent driving voltages (8 drivers) are used to drive the 1024 nozzles. Note that the use of shared drivers for driving many nozzles (e.g., 128 nozzles per driver) has been common because of the advantage of cost reduction regarding driver electronics. In the SG1024 head, one module consists of two adjacent nozzle rows and one head comprises four modules, as shown in Fig. 1(b). In terms of the driver electronics, one module corresponds to one 256-nozzle head (Q-class, Fujifilm Dimatix, U.S.A.). Note that the previous method used only a single circuit and only one data-acquisition channel to monitor a Q-class (256 nozzles) printhead.[13] In this study, we used four self-sensing circuits and four channels for the data acquisition to monitor the four modules of 256 nozzles each. Here, the critical issue is to develop the algorithm for a fast scanning of all

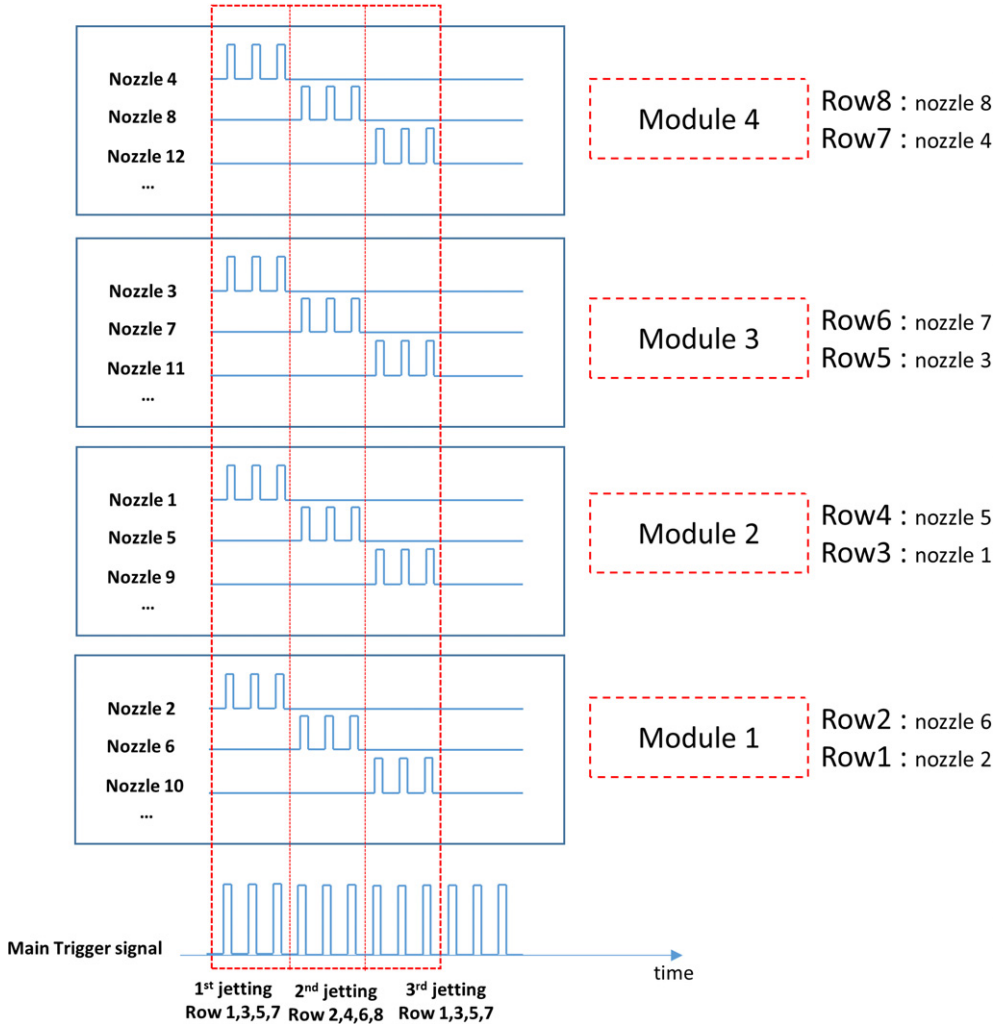

Figure 2. Parallel scanning scenario for $N_{ave} = 3$.

the nozzles irrespective of the number of nozzles, modules, and heads. To better explain the proposed parallel scanning method for fast scanning, we present an example using three-time averagings ($N_{ave} = 3$) for each nozzle without loss of generality, as illustrated in Figure 2. To average the self-sensing signals, the repeated jetting of each nozzle was used to acquire the repeated self-sensing signal. Note that each jetting trigger should be used for the data acquisition.

It is important to make sure that one nozzle in each module should be jetted (or excited for pressure-wave generation) to monitor that particular nozzle. Otherwise, signals from other nozzles will appear in the measured signal, and the jetting status of a specific nozzle cannot be detected.[12] As a result, for the SG1024 head, up to four nozzles can be simultaneously jetted for scanning purposes. Fig. 2 shows the jetting scanning scenario to minimize the scanning time by jetting four nozzles from each module simultaneously. For the example of three averagings, the first three triggers will jet four nozzles (1,2,3,4) simultaneously while the other nozzles are turned off. The next three triggers will jet the next four nozzles (5,6,7,8) simultaneously. As a result, the total number of jetting triggers can be reduced, and the time required to scan all 1024 nozzles is equivalent to that for 256 nozzles. The required scanning time, T_{scan}, for 1024 nozzles can be written as follows:

$$T_{scan} = (N_{ave} * 256)/F. \quad (1)$$

Here, the scanning frequency, F, is fixed throughout the scanning process, and the jetting nozzles are switched in order to scan all the nozzles according to the scanning scenario during the time intervals between jetting triggers.

The sequential scanning scenario described in Fig. 2 is similar to the bitmap printing of a specific pattern. Therefore, the scenario-based parallel scanning scenario can be easily implemented for any printing driver by uploading the printing data (a bitmap) that will generate scanning jetting according to externally or internally generated triggers. Note that the trigger signal for scanning is not generated by the encoder of the motion stages, but is internally generated at a setting frequency that is different from that of the printing process.

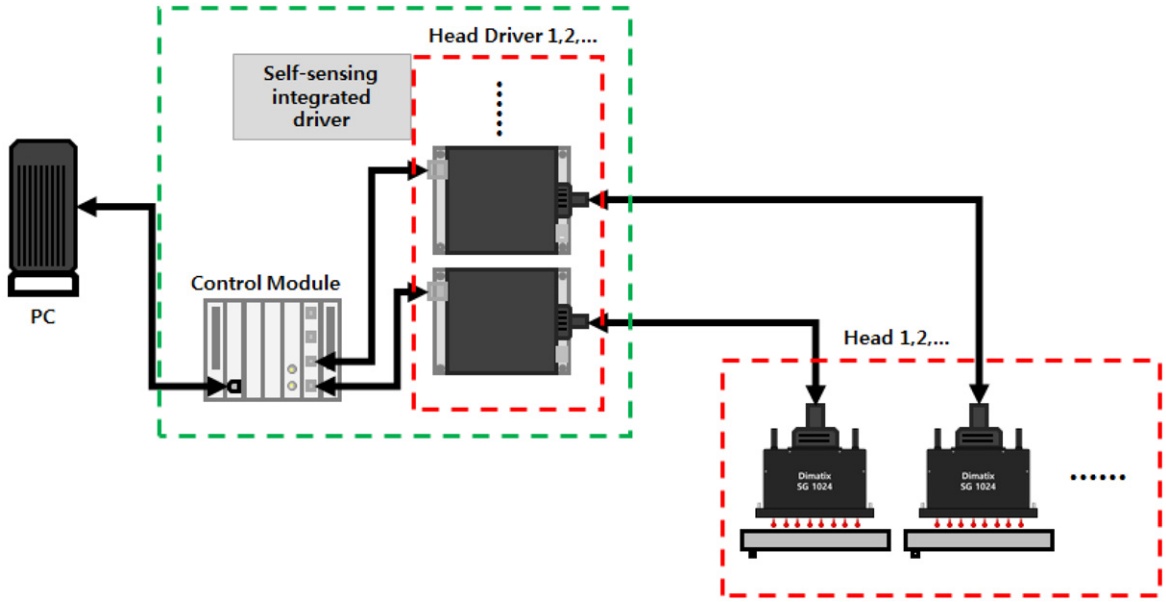

Figure 3. Schematic for printing driver configuration with self-sensing capability.

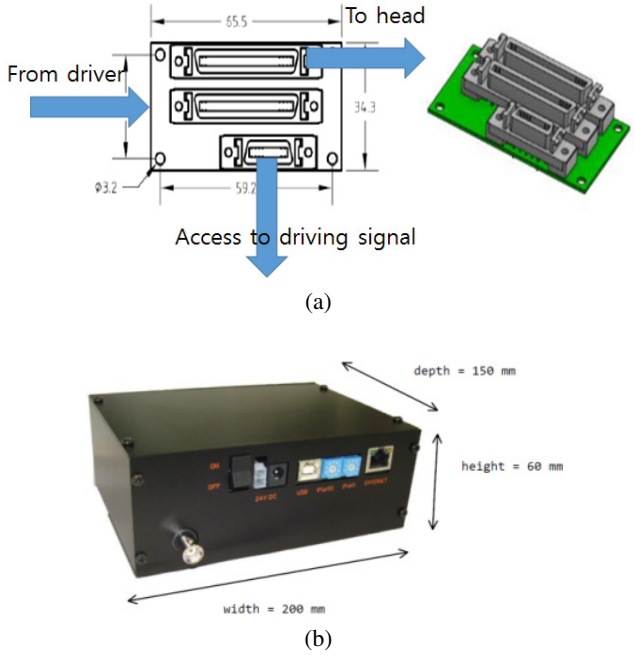

Figure 4. Prototype of external module. (a) Connector to access the driving signal from the SG1024. (b) External module.

It is always recommended to use a higher scanning frequency for faster scanning of all the nozzles. However, a scanning frequency limitation also exists because of the data-acquisition necessity. In this study, 100 data samples ($N_{\text{data}} = 100$) were acquired per jetting trigger signal (data-acquisition trigger) with a sampling rate of 1 mega samples per second (MS/s). For this data-acquisition time, the scanning frequency should be lower than 10 kHz.

The generated pressure wave inside a head will not fully decay before the next jetting trigger when the jetting frequency is high[15–17] consequently, the sensing signals could be different according to the scanning frequency. In this study, a scanning frequency of $F = 9$ kHz was used throughout the experiment. For a fixed scanning frequency, the number of averagings (N_{ave}) is the only factor that can affect the total scanning time, T_{scan}, as discussed in Eq. (1). However, if the number of averagings is reduced, the diagnosis can be less accurate if there is electrical noise. Considering the trade-off, 10 averagings ($N_{\text{ave}} = 10$) were used; so the total scanning time for the scanning of the 1024 nozzles is 0.28 seconds. During the scanning process, the sampled sensing data were stored in the memory of each module in sequential order. The amount of sampled data after scanning would be $N^*_{\text{ave}}1024^*N_{\text{data}}$ where $N_{\text{ave}} = 10$ and $N_{\text{data}} = 100$. The repeated sensing data of each nozzle were averaged in the firmware so that the data requiring data transfer to a PC for further analysis could be reduced to 1024*100. Note that we did not use the first several dozen sampled data out of each 100 in the detection algorithm, because initial sensing signals are likely to be affected by the driving signal.

To detect the jet failures using the self-sensing signals, the reference signals, measured at normal jetting conditions, x^r_k, had to be compared to the monitoring signal, x^m_k. Here, the reference signals represent the normal jetting condition, and we had eight different reference signals, since the SG1024 head comprises eight independent drivers.

To calculate the nozzle status, two different methods can be used: (1) the cosine value of two signals, or (2) the variance value.[12,13]

The cosine value of each nozzle between the reference and monitoring signals (or vectors), C_k, of the nozzle number, k, is defined as follows:

$$C_k = \frac{x^r_k \cdot x^m_k}{|x^r_k|\,|x^m_k|}. \tag{2}$$

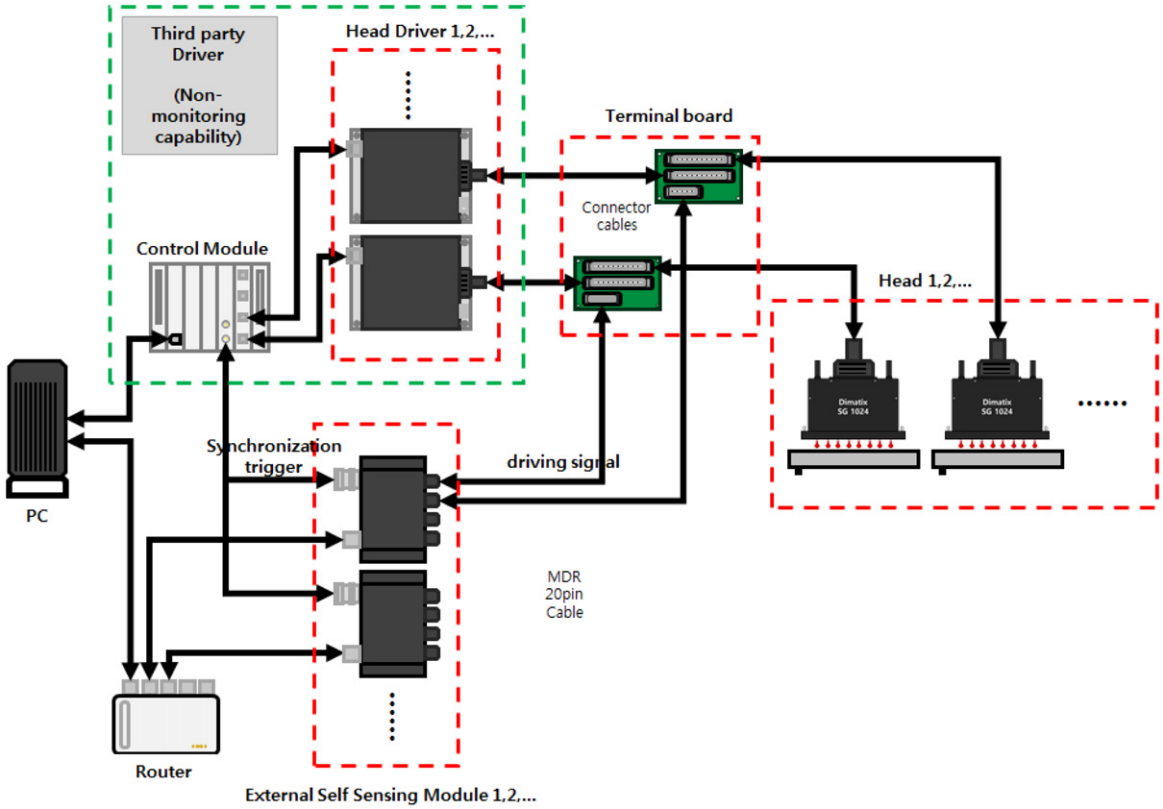

Figure 5. Schematic for multi-head monitoring using an external sensing module.

Note that the ·(dot) represents the dot product of two vectors. Here, $k = 1, 2, \ldots, 1024$, since there are 1024 nozzles. The cosine value of Eq. (2) mainly detects the phase change in the self-sensing signal with respect to the reference signal. For example, if the phase difference is zero, the value becomes 1. However, if the phase difference increases and becomes close to 180°, the value becomes −1. The cosine value in Eq. (2) can also detect a frequency change of the signals. If the frequencies of the two compared signals are not the same, the value is close to 0. The use of cosine value has additional advantages, because the cosine value can easily be normalized from −1 to 1 depending on how close the signals are. Also, the method is less affected by electrical noise, which is not related to the pressure-wave signal. However, the method cannot detect the jet failures that affect only the magnitude of a signal without changing its phase. So, additional methods should be used to detect all jetting failures. On the other hand, the variance value, V_k, has been used for detecting inkjet malfunctions based on the self-sensing signals.[12] The variance value can be defined as follows:

$$V_k = \sum_{j=1}^{N} [x_k^r(j) - x_k^m(j)]^2. \quad (3)$$

Here, N represents the number of the sampled self-sensing data. We used $N = 60$ to exclude the first 40 data from the sampled data ($N_{\text{data}} = 100$). V_k was compared to a threshold value in order to judge the jetting status. The main advantage of using Eq. (3) is that a slight variation of the self-sensing signal can be effectively detected. The drawback of Eq. (3) is that the monitoring results can easily be affected by electrical noise.

Since the two different methods in Eqs. (2) and (3) have their own advantages, the accuracy of the monitoring results can be improved by combining them. In this study, we propose a new judgment criterion based on the two existing criteria as

$$D_k = A_1 * C_k + (A_2)/(A_3 V_k + 1). \quad (4)$$

Note that the scale factors for each criterion (A_1, A_2, A_3) should be considered, because V_k differs from C_k. For example, the smaller value of V_k close to zero indicates normal jetting status, while a larger value of C_k close to the maximum value of one ($C_k \approx 1$) indicates normal jetting status. To make higher values for better conditions, the inverse of V_k should be used. Here, to avoid possible division by zero, the constant value of one is added. A scale factor of A_3 is used to balance the constant value of one and V_k. Also, the weighting factors of A_1 and A_2 are used so that the maximum value of D_k can be 100, to make it easier to understand the degree of malfunction.

Self-sensing module prototype development

For the practical implementation of the proposed monitoring methods, we developed two different prototypes: (1) a driver

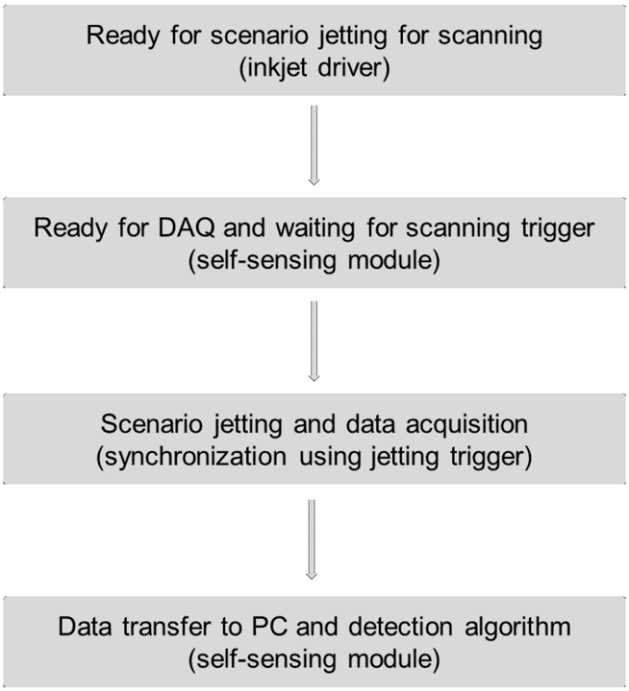

Figure 6. Flow chart for self-sensing measurement.

integrated module and (2) an external module for third-party drivers.

Since the hardware requirement for the self-sensing module is relatively simple, it can be integrated into the inkjet driver. Since most inkjet drivers are designed for multi-head printing, the sensing modules integrated into the driver unit can be easily extended to monitor multiple heads simultaneously. For example, the proposed printing controller can install eight printer driver control module slots, and each slot has four sockets for head drivers. As a result, 32 heads are supported for simultaneous printing and monitoring. Figure 3 shows the schematic of the inkjet driver configuration with the self-sensing capability. It has a zero form factor for the monitoring module, which is desirable for most inkjet applications.

Despite the advantages of the self-sensing integrated driver module, most printing-system developers may prefer their own printer drivers according to their requirements. So, we developed another prototype, where the SG1024 jetting can be monitored no matter what inkjet head driver is chosen. In the SG1024, there is a 60-pin connector to which all the external devices are attached. The connector is located on the top side of the head. For an easy access to driving signals from the connector, we designed an additional cable connector, which can be easily inserted between the driver and the head, as shown in Figure 4(a). The connector has one cable input from the driver and two cable outputs for the head and the self-sensing module, as shown in Fig. 4(a). The cable output port for the head has the same connector-pin layout as the input port from the driver, so the original signal from the driver is unchanged. In this way, we could access the driving signal to get the self-sensing signal without interrupting the

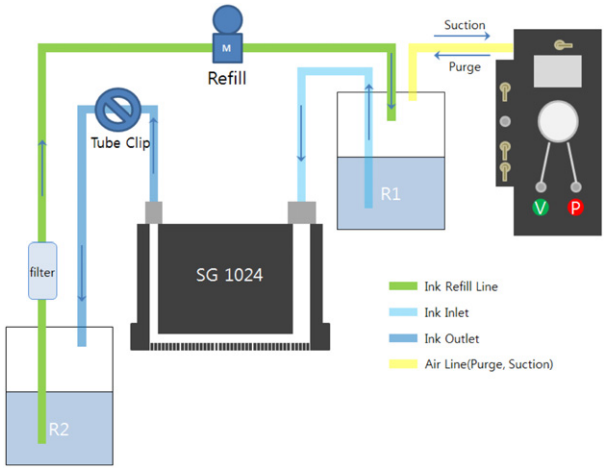

Figure 7. Schematic of the fluidic system for the SG1024.

driving signal for the printhead. Note that the method for extracting the self-sensing signals from the driving voltage has been discussed in Ref. 12.

By using the connector shown in Fig. 4(a), the driving signals from the eight drivers can be accessed for the external module shown in Fig. 4(b). The external module is designed to monitor dozens of printheads simultaneously. For this purpose, it has an Ethernet connection to a PC, and each module has its own IP address via a rotary DIP switch to address and monitor 99 heads simultaneously. Note that the monitoring system using external modules could be bulky if the number of heads to be monitored increases. In addition, there is an issue of handing external cables when monitoring many heads. For example, cables for PC communication, electrical cables to access the driving signals, and trigger cables to synchronize the jetting and data acquisitions are required. In addition, if the cables are too long, there can be electrical noise in addition to the difficulties of handling cables. Figure 5 shows a head driver and monitoring module configuration for multi-head systems. As shown in Fig. 5, the configuration was much more complex than the self-sensing integrated module shown in Fig. 3.

Note that to get the self-sensing data, the data acquisition had to be synchronized with the jetting trigger signal from the driver. Figure 6 shows a flow chart for self-sensing data measurement. As a first step, the parallel scenario jetting data are uploaded in the driver, so that the scanning process is in a ready status. Then, we set the data acquisition ready so that it can be in waiting status for the data-acquisition trigger. When both the head driver and the monitoring module are ready for scanning and data acquisition, the parallel-based jetting scenario is started. Then, the data acquisition will acquire signals based on the jetting trigger. Note that the trigger signal of parallel scenario jetting is connected to the input trigger of the external module for data acquisition. Here, we are using the total number of 2560 triggers; each trigger has an interval of about 111.11 μs (inverse of 9 kHz) to scan 1024 nozzles with 10 averagings. The data-acquisition system acquires 100 data per each trigger, and the data

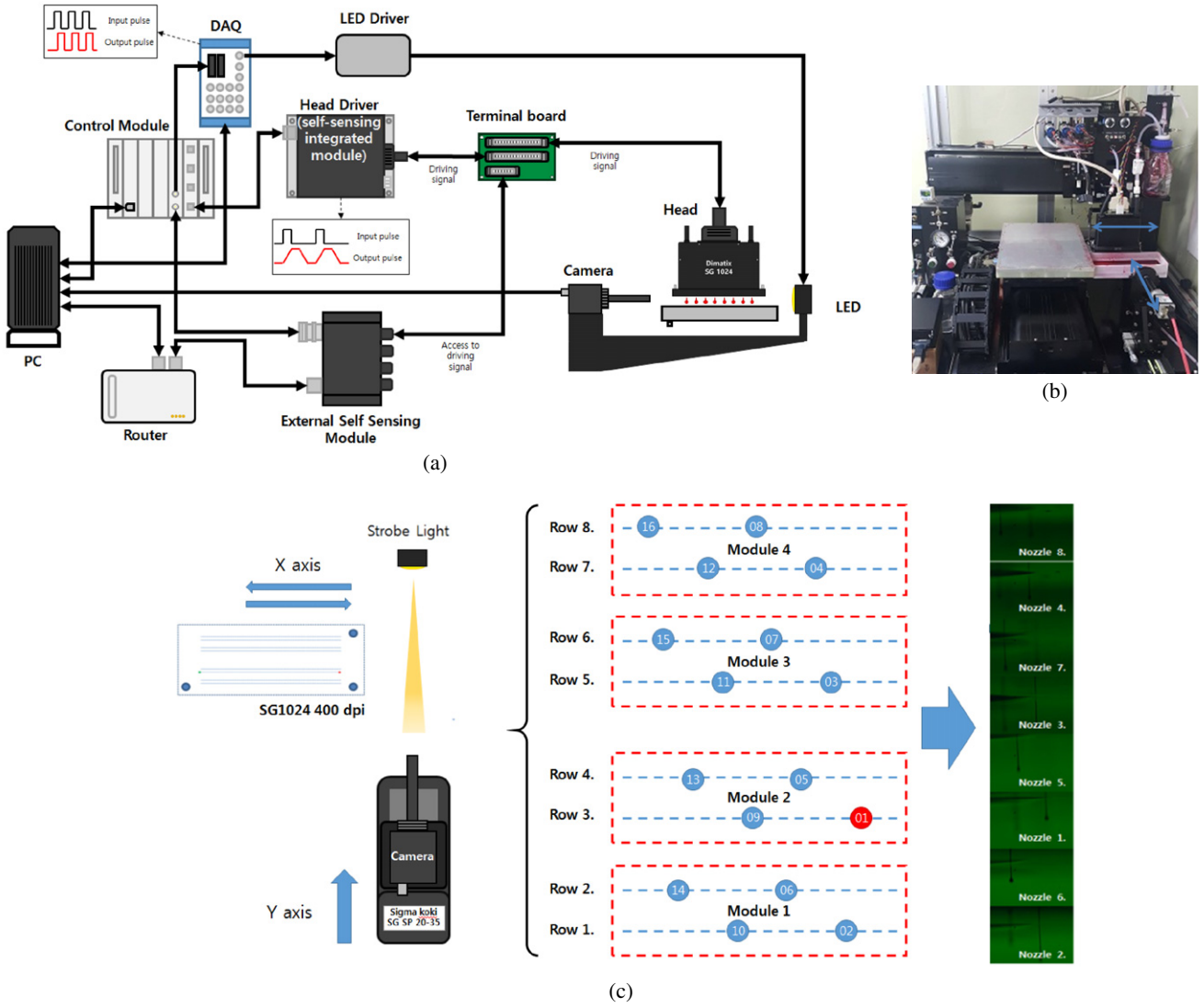

Figure 8. Drop visualization system for the SG1024. (a) Schematic for the SG1024 monitoring system. (b) Photo of the hardware for the drop visualization. (c) Camera positioning for each nozzle.

is stored in the sensing module's memory before being transferred to the PC.

The sensing algorithm shown in Fig. 6 can be carried out simultaneously for driving many heads. As a result, our proposed parallel (independent) sensing algorithms can scan all nozzles within 1 second no matter how many heads there are.

Experimental verification

To verify our self-sensing system, a drop-watcher system for the SG1024 head was developed. To supply ink to the SG1024, we designed a fluid recirculation system, as shown in Figure 7. The recirculation allows for quicker priming times, helps maintain inks that are prone to sedimentation, and keeps the printhead wetted when handling quick drying inks. We found that the use of the fluid recirculation system increased the jetting reliability[14]. As shown in Figure 8, we used two ink reservoirs for recirculation: one is the main ink tank, which is indicated as R2; the ink in R2 is collected from the outlet of the head. The reservoir indicated in R1 supplies ink to the head via a hydrostatic force (fluid height difference). Therefore, the reservoir R1 should be positioned slightly above the inkjet head, while the main reservoir R2 is positioned below the printhead to allow the recirculation. In this way, unused ink in the head returns to the main tank (R2). In the inkjet reservoir (R1), there is a fluid level sensor. If the ink level in R1 becomes low, the fluid pump will pump ink from R2 to refill R1 to the target level.

To avoid the dripping of ink from the head, a slight negative pressure, generated by a pneumatic module, is applied to the ink reservoir, in order to maintain proper meniscus for jetting. In addition, the pneumatic module can generate strong positive and negative pressures as needed for maintenance.

To verify the monitoring capability of the self-sensing signal, a strobe light emitting diode (LED) was used to visualize the jet images from a charge-coupled device (CCD) camera. The LED light was synchronized with the jetting trigger to obtain frozen images from the CCD camera. The

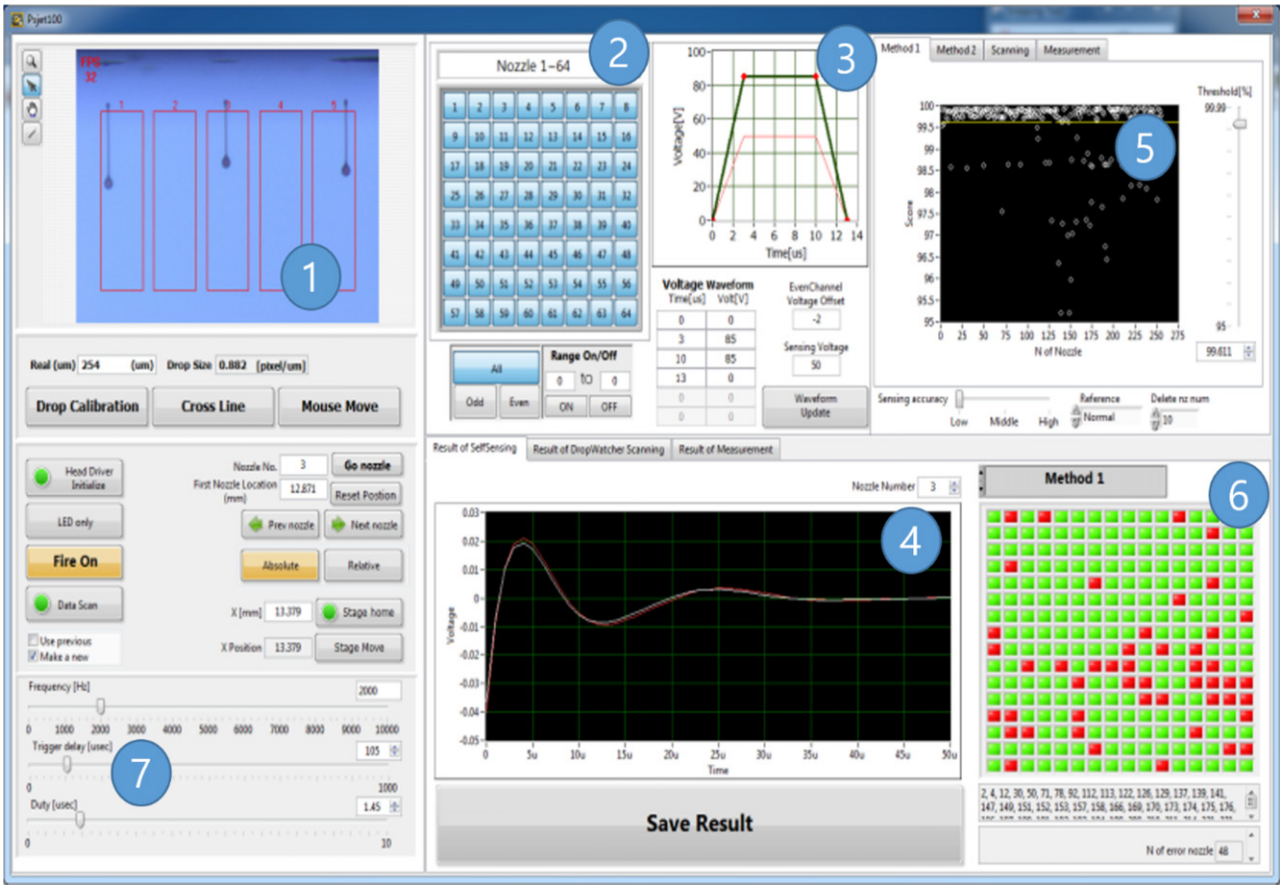

Figure 9. Monitoring software for setup. (① Image display for the jetting image, ② Menu for nozzle selection, ③ Waveform editor, ④ Comparison of self-sensing signals, ⑤ Score value of D_k ⑥ Nozzle-status indicator and ⑦ Strobe LED control).

detailed information on drop visualization can be referenced in Ref. 1.

Fig. 8 shows the experimental setup for the monitoring of the SG1024. Since the head has eight rows and each row has 128 nozzles, the camera focus should be moved toward the head (y direction) as well as in the x direction in order to acquire jetting images from a specific nozzle. For this purpose, we used a motorized stage (SG SP 20-35, Sigma Koki, Japan) to control the camera location in the y direction to monitor the nozzles in the different rows. We also used a linear stage to locate nozzles in the x-direction (the nozzles in a row). In this way, jetting from all nozzle locations could be monitored in both directions, as shown in Fig. 8(c).

As shown in Fig. 8(c), all nozzles are numbered so that each row has an eight-number increment and the adjunct-number nozzles are located in different rows. To capture the droplet image of a specific nozzle, the location of each nozzle should be calculated and stored in advance for the positioning control of the motorized stages.

To demonstrate our two prototypes of self-sensing modules, two modules were connected, as shown in Fig. 8(a), so that both module prototypes could be tested. With this configuration, the self-sensing signals from either one module or both could be compared. From the comparison of the two modules, it was confirmed that the self-sensing signals can be equally measured for both modules. In this article, we use the self-sensing signals from the internal module to explain our real-time monitoring software.

To demonstrate our system, we developed jetting monitoring software, which can show and update the current nozzle status based on the measured self-sensing signal as shown in Figures 9–12.

For the experiment, standard ink from Dimatix (XL-30, Dimatix, U.S.A.) was used throughout the experiment. The viscosity of the ink is approximately 14 cP at 24^{deg}C.[13] If other inks are used for the monitoring process, the reference signal of the specific ink should be stored in advance to detect any monitoring signal deviation from the reference signal, which can be easily calculated by averaging the self-sensing signals of all nozzles in the same row.

Fig. 9 shows the software for adjusting the parameter setup for the self-sensing prior to the real-time monitoring. For the jetting verification, we used the image display shown in Fig. 9① to show the jetting image of a specific nozzle. To visualize the jetting from a specific nozzle, the motorized stages was moved so that the camera could observe the jetting. To obtain the frozen images, the strobe LED light should be synchronized and the lighting delay with respect to jetting signal can be adjusted from the menu shown in Fig. 9⑦. Fig. 9② shows the nozzle selection menu for the

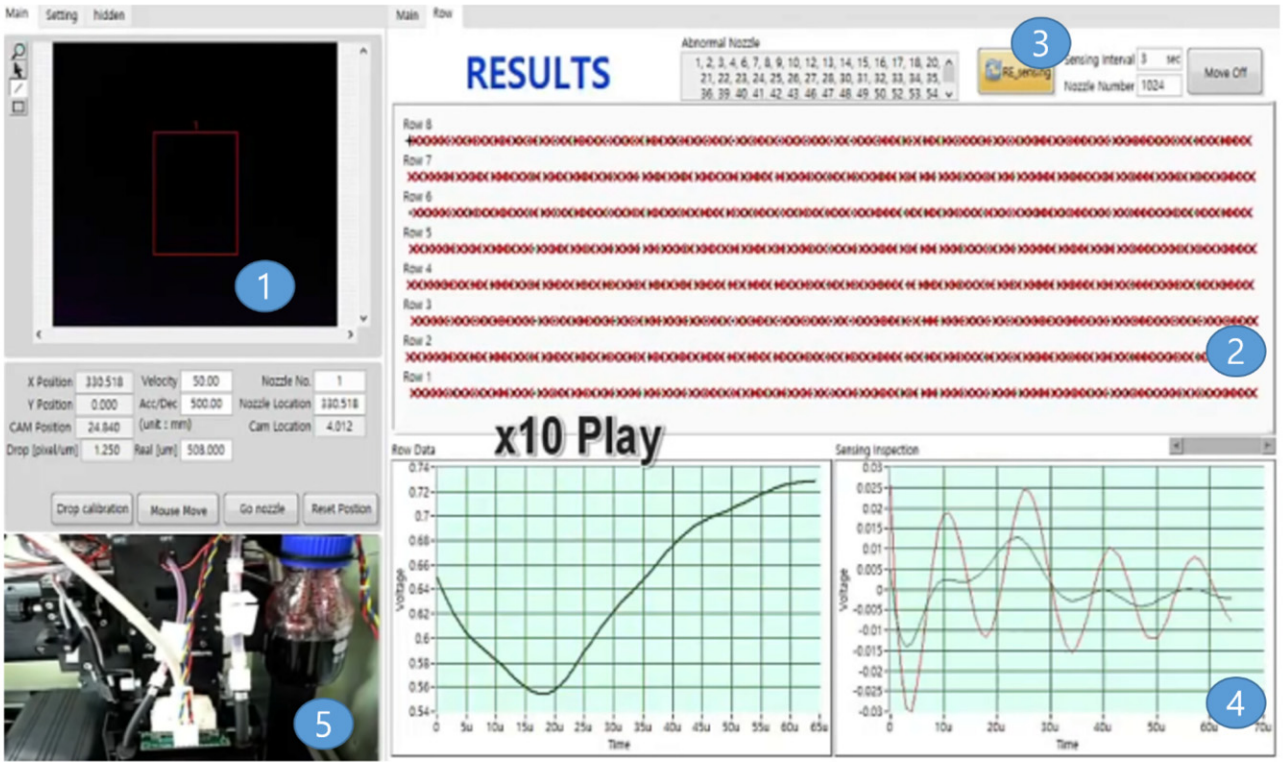

Figure 10. Real-time jetting monitoring results when ink is removed from head. (① Image display, ② Nozzle layout for the 1024 nozzles, ③ Real-time monitoring selection, and ④ Self-sensing signal comparison).

selection of the Boolean switch to turn the nozzles on (or off), and it can also be used as an indicator of whether a specific nozzle has been selected for jetting.

Fig. 9③ shows the waveform editor for the driving voltage. Note that we can set up two different voltages for the jetting and the sensing. In this experiment, 85 V was used for the jetting. However, for the nozzle-status scanning based on the self-sensing signal, we used a voltage of 50V, which did not produce any jetting. Note that the detection of a faulty nozzle by the self-sensing signal is based on the pressure-wave propagation in the ink and does not require actual jetting. The use of a non-jetting low voltage for monitoring has advantages because it does not contaminate the substrate during the monitoring process.

In the initial scanning, we calculated the reference data (averaged signal) based on the current-sensing signal data, and each nozzle was compared to the reference signal to determine the nozzle status. By using the reference data, each nozzle status could be displayed as a Boolean indicator, as shown in Fig. 9⑥. Here, the results for only one module of the 256 nozzles are shown in Figs. 9⑤ and ⑥, because of the limitation of space in the software. We recommend that more than 70% of the nozzles should be in good condition to get reasonably good reference data. If more than 30% of the nozzles are not in good condition, proper maintenance should be performed until most of the nozzles become jettable.

Fig. 9④ compares the self-sensing data and the reference signal by overlapping the two signals on a graph. The sensing signal shown in Fig. 9④ is the averaged data for 10 times that have been digitally filtered to remove the possible electrical noise. Note that we used 60 data out of 100 for the comparison using Eq. (4) by cutting off first 40 data, which may have been affected by the driving voltage. The monitored signal can be scored using Eq. (4) according to the closeness to the reference signal. The score for each nozzle, D_k, can be plotted, as shown in Fig. 9⑤. By setting up threshold values that range from 0 to 100, the nozzle with a score lower than the threshold value can be classified as faulty nozzle, which needs maintenance. The score values for most of the non-jetting nozzles are less than 80 but the normal nozzle values are close to 99. Considering the score values of both jetting and non-jetting nozzles, the threshold value of 95, which is slightly less than the score values of most of the normal cases for the detection of most malfunctioning nozzles, was selected.

After the initial setup of the parameters, real-time monitoring during printing was needed. Figs. 10–12 show the software for the real-time monitoring. Here, the sensing results were regularly updated at the setting intervals. For example, if we set a sensing interval of 3 seconds, the monitoring results of all nozzles were updated every 3 seconds. In an actual printing system, the monitoring should be done during short non-printing idle times, so that the interruption of the printing process by the monitoring can be minimized. It is desirable to be able to identify the problematic nozzles at a glance. For this purpose, the nozzle layout of the head was used to indicate the nozzle status, as

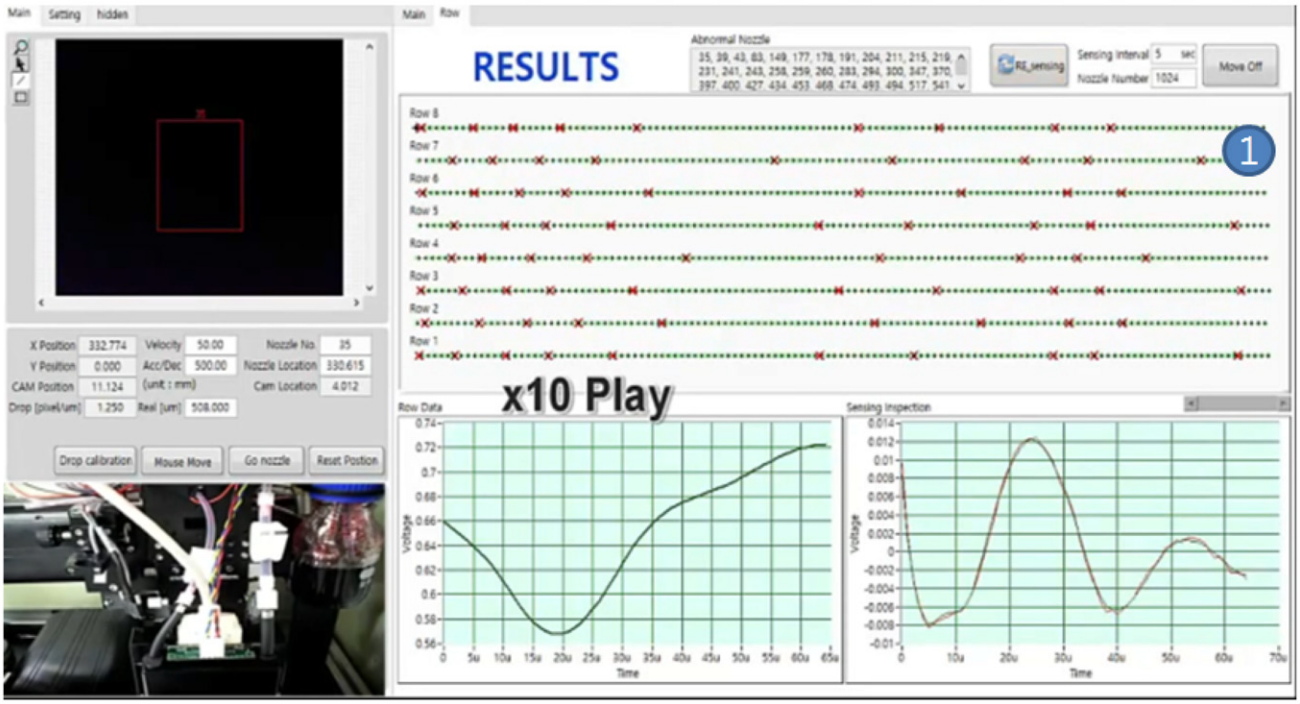

Figure 11. Real-time jetting monitoring results after a few seconds of recirculation.

shown in Fig. 10③. Here, the location of a faulty nozzle is shown as a red "x," whereas a green dot is used for the normal nozzles.

For verification of the monitoring results, the nozzle locations in Fig. 10② can be selected by a mouse click to show the jetting images in the image display in Fig. 10①. For a comparison of the monitored signal and the reference signal, the self-sensing signals of the selected nozzle are shown on the graph in Fig. 10④.

We tested two different inkjet malfunction cases: (1) no ink inside the inkjet head (the ink was drained from the head) and (2) a nozzle surface blockage. For better understanding of the malfunction, we took videos of the two abnormal cases, as shown in Fig. 10⑤ and they were compared with the nozzle status in Fig. 10②.

Fig. 10② shows the monitored jetting status when the ink was removed from the head. As shown in Fig. 10②, most of the nozzles became non-jetting, indicated as a red "x" in the nozzle map. Note that the fluidic supply system for the SG1024 can recirculate the ink, enabling some of the nozzles to return to the normal status.

By using real-time monitoring, it was possible to observe the whole process of the jetting status recovery during ink circulation. Fig. 11 shows the monitored jetting status after a few seconds of the recirculation, when more than half the nozzles had recovered. To confirm the monitoring results, a nozzle in Fig. 11① can be selected to show its jetting image using a mouse click. In this way, the monitored results can be verified. Readers may refer to the video in Ref. 18 for better understanding of the real-time monitoring in relation to the fluidic system. Note that not all nozzles were recovered through the use of only the recirculation process; maintenance schemes, including strong purges, may be needed to fill the ink in the inkjet channel for the unrecovered nozzles. The monitored signal can also be used to check whether all of the nozzles are jetting normally after the maintenance process.

As another example of detecting jet failure, we used our fingers to block the head in the y direction, as shown in Fig. 12①. Experimental results showed that nozzle blockage and location can be identified in real time. We observed from our experiment that most of the non-blocked nozzles became normal after the fingers were removed from the nozzle surface.[18]

CONCLUDING REMARKS

To monitor a commercial head with 1024 nozzles, we developed monitoring modules, which use parallel sensing schemes to minimize the scanning time.

The modules are designed to monitor multiple heads simultaneously and take less than 1 second to scan 1024 nozzles. A software algorithm for determining nozzle status has been proposed so that robust monitoring results can be obtained from the acquired sensing data. The experiment results showed that the jetting status for all 1024 nozzles was successfully updated in real time. If any faulty nozzles were detected via real-time monitoring, the faulty nozzle could be corrected by proper maintenance, including purging and wiping the nozzle surface. Our proposed real-time monitoring methods can also be used to determine whether all nozzles have become normal via the maintenance scheme. As a result of real-time monitoring after maintenance, the

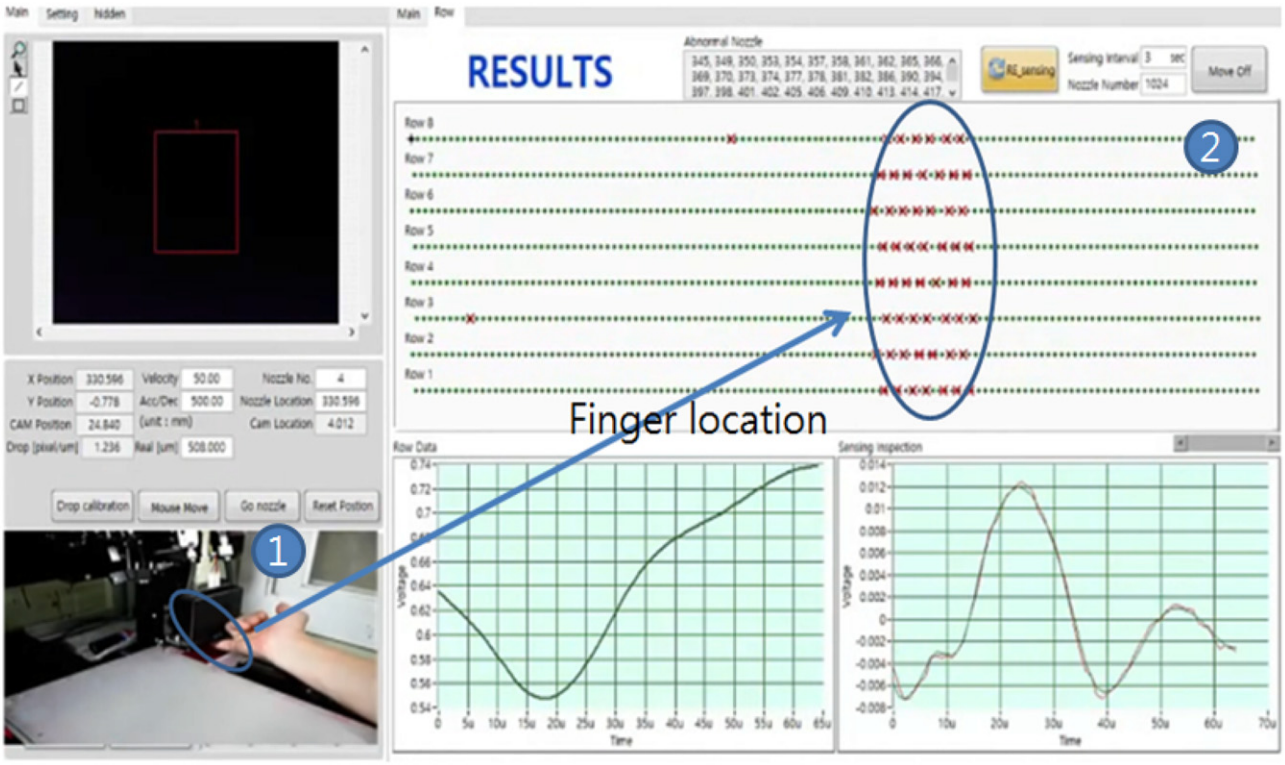

Figure 12. Real-time jetting monitoring results of nozzle blockage (① Blocked location and ② Self-sensing result).

time and effort needed for maintenance can be significantly reduced. This could be another benefit of using our self-sensing-based jetting status monitoring. As a future work, multi-head monitoring will be implemented using the developed modules of the present study.

ACKNOWLEDGMENT

This research was supported by the Commercializations Promotion Agency for R&D Outcomes (COMPA) funded by the Ministry of Science, ICT, and Future Planning (MSIP) and partially supported by the Soonchunhyang University Research Fund.

REFERENCES

[1] K. S. Kwon, "Vision Monitoring," in *Inkjet-Based Micromanufacturing*, edited by J. G. Korvink, P. J. Smith, and D.-Y. Shin (Wiley-VCH Verlag GmbH & Co., KGaA, Weinheim, Germany, 2012), chap. 9.

[2] H. Ujiie, "State of the art of digital textile printing status 2014," *Proc. NIP30: 30th Int'l. Conf. on Digital Printing Technologies and Digital Fabrication 2014* (IS&T, Springfield, VA, 2014), pp. 2–2.

[3] H. Shinada, "Single-pass inkjet digital printing technology for commercial printing markets," *Proc. NIP28: 28th Int'l. Conf. on Digital Printing Technologies and Digital Fabrication 2012* (IS&T, Springfield, VA, 2012), pp. 2–5.

[4] H. Dong, W. W. Carr, and J. F. Morris, "Visualization of drop-on-demand inkjet: Drop formation and deposition," Rev. Sci. Instrum. **77**, 085101 (2012).

[5] A. Famili, S. A. Palkar, and W. J. Baldy Jr., "First drop dissimilarity in drop-on-demand inkjet devices," Phys. Fluids. **23**, 012109 (2011).

[6] K. S. Kwon, M. H. Jang, H. Y. Park, and H. S. Ko, "An inkjet vision measurement technique for high frequency jetting," Rev. Sci. Instrum. **85**, 065101 (2014).

[7] T. J. Abrott, "Systems and methods for verifying the operational conditions of print heads in a digital printing environment", US Patent, US 20080079763 A1 (2006).

[8] D. J. Forrest, J. C. Briggs, M.-K. Tse, and S. H. Barss, "Print quality analysis as a QC tool for manufacturing inkjet print heads," *Proc. NIP14: 14th Int'l. Conf. on Digital Printing Technologies* (IS&T, Springfield, VA, 1998), pp. 328–674.

[9] A. J. Ahne and B. K. Owens, "Faulty nozzle detection in an ink jet printer by printing test patterns and scanning with a fixed optical sensor", US Patent 6637853 B1 (2003).

[10] J. D. Jong, R. Jeurissen, H. Borel, M. V. D. Berg, H. Wijshoff, H. Reinten, M. Versluis, A. Prosperetti, and D. Lohse, "Entrapped air bubbles in piezo-driven inkjet printing: Their effect on the droplet velocity," Phys. Fluids **18**, 121511 (2006).

[11] R. Jeurissen, J. D. Jong, H. Reinten, M. V. D. Berg, H. Wijshoff, M. Versluis, and D. Lohse, "Effect of an entrained air bubble on the acoustics of an ink channel," J. Acoust. Soc. Am. **123**, 2496 (2008).

[12] K. S. Kwon, Y. S. Choi, D. Y. Lee, J. S. Kim, and D. S. Kim, "Low-cost and high speed monitoring system for a multi-nozzle piezo inkjet head," Sens. Actuators A **180**, 154 (2012).

[13] K. S. Kwon, Y. S. Choi, and J. K. Go, "Inkjet failures and their detection using piezo self-sensing," Sens. Actuators A **201**, 335 (2013).

[14] W. Zapka, S. Pausch, and H. P. Rapp, "Improved reliability in industrial inkjet printing," *Proc. NIP24: 24th Int'l. Conf. on Digital Printing Technologies and Digital Fabrication 2008* (IS&T, Springfield, VA, 2008), pp. 865–868.

[15] K. S. Kwon, "Waveform design methods for piezo inkjet dispensers based on measured meniscus motion," J. Microelectromech. Syst. **18**, 1118 (2009).

[16] D. B. Bogy and F. E. Talke, "Experimental and theoretical study of wave propagation phenomena in drop-on-demand ink jet devices," IBM J. Res. Development **28**, 314 (1984).

[17] K. S. Kwon and W. Kim, "A waveform design method for high speed Piezo inkjet printing based on self-sensing measurement," Sens. Actuators A **140**, 75 (2007).

[18] K. S. Kwon, "SG1024 inkjet jetting failure monitoring," https://youtu.be/AGdDRxP-Bf0.